A Single-Shot, Multiwavelength Electro-Optic Data-Acquisition System for Inertial Confinement Fusion Applications

Introduction

On large inertial confinement fusion (ICF) laser systems like the National Ignition Facility (NIF),[1] the signals from diagnostic instruments originate in an environment where the ionizing radiation and electromagnetic interference (EMI) can significantly degrade the signal-to-noise ratio (SNR) of the measurement or even damage the recording equipment. In addition, there are many recording channels to which these considerations must apply. The cost of the recording system can be reduced if the signals from several detectors can be multiplexed together onto a single, protected oscilloscope channel. Modern high-bandwidth oscilloscopes have nearly infinite record lengths that make this serial multiplexing possible. The prototype system described here is focused on the set of 36 vacuum x-ray photodiodes (XRD's) of the NIF Dante instruments[2] that produce temporally resolved x-ray spectra.

In high-EMI environments, an electro-optic (EO) data-acquisition system is desirable. Fiber optics provide a means of isolating the recording equipment from the harsh detector environment. The signals from the XRD's are converted into the optical domain with fiber-optic Mach–Zehnder modulators (MZM's).[3] The MZM's are typically built to telecom specifications that make it possible for them to survive not only voltage transients of 250 V for 1 μs (Ref. 4), but also the EMI in an ICF environment and the maximum output of an XRD. Once the signals are in the optical domain, they can propagate on single-mode optical fiber that provides high-bandwidth (BW) transmission over long distances. The BW of the fibers is much larger than the signals being recorded, so arbitrarily long fiber delays can be added to the signal paths. These long delays, coupled with wavelength-selective fiber-coupling techniques, allow one to serially combine multiple signals onto a single photodetector.

The system described here was designed as a prototype for the NIF Dante instruments. These instruments use XRD's to measure the x-ray spectra of ICF implosions. There are 36 channels spread over two instruments. The specifications require that signals be acquired in a temporal window at least 200 ns

long. The response time of the XRD's is 120 ps, so the system requires a minimum BW of 2.75 GHz. The system was actually designed to a 6-GHz BW to accommodate multifringe events, which will be discussed later. The XRD's can deliver a maximum unsaturated signal of 200 V. The minimum meaningful signal is 50 mV and the desired SNR at this level is 5, which implies a dynamic range (DR) of greater than 4000:1. This DR exceeds the capabilities of the current electronics. With this newly adopted requirement the instrument will be able to record signals without changing any radio-frequency (rf) attenuators.

Experimental

This data-acquisition system is designed to operate in the near-IR optical C band with wavelengths from 1530 nm to 1560 nm, which are used by the telecommunications industry. A layout of the system is shown in Fig. 130.89. The optical carriers are provided by continuous-wave (cw), fiber-coupled laser diodes (LD's) that use distributed-feedback Bragg gratings to maintain narrow-bandwidth operation. The International Telcommunication Union (ITU) has specified a standard set of wavelengths separated by approximately 1.6 nm (200 GHz) around which telecom components are fabricated.[5] The output power of these types of devices ranges from 20 to 100 mW (13 to 20 dBm) with a typical noise figure of –140 dB/Hz. The prototype system used a 20-mW LD at 1552 nm and a 60-mW LD at 1557 nm. The 20-mW version is less expensive and more readily available at all wavelengths on the ITU 200 grid. The 60-mW laser is better suited to compensate for losses in the system. However, cw illumination is inappropriate for this application because of the requirement to multiplex signals. The cw wings of the serially combined signals would overlap, thereby overwhelming the photodetector or forcing a reduction of the signal amplitude by N, the number of serially overlapped signals.

The cw lasers are converted into pulsed lasers via acousto-optic modulators (AOM's). These optical modulators have very high contrast ratios (50 dB) with a rise time of 10 ns. They also allow for both digital and analog modulation. In the prototype described here, the AOM's produced pulses that were 40 ns
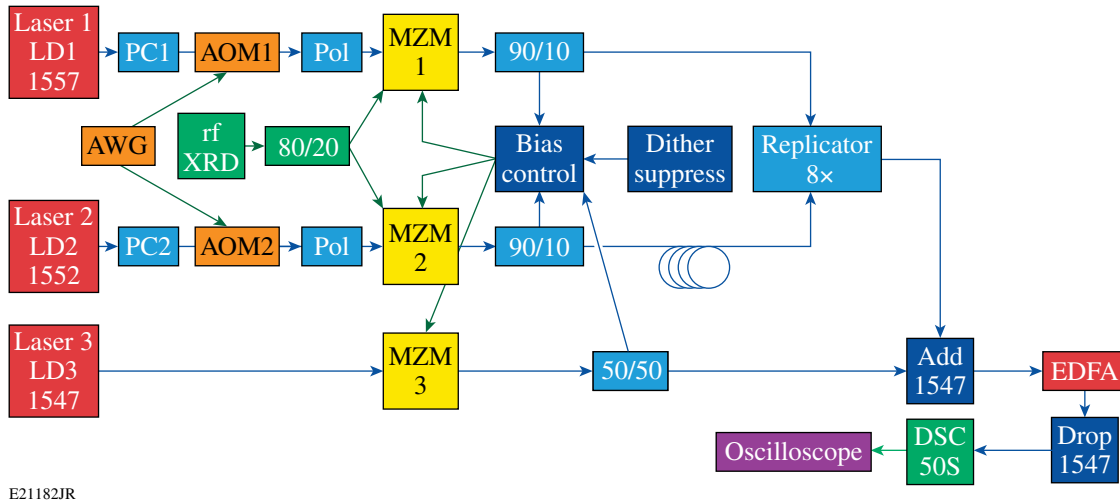
E21182JR

Figure 130.89
In the EO data-acquisition system, the cw outputs of LD1 and LD2 are pulse shaped with an AOM with the shaping pulse provided by the arbitrary waveform generator (AWG). The light is polarized (pol) before being modulated by the MZM. The MZM's are driven by a single XRD through an 80/20 splitter. The 90/10 splitters provide an optical feedback signal to the bias control loop. The signals from the two MZM's are combined at the input of the 8× replicator. After the replicator, another cw source (LD3) is added to provide a cw input to the EDFA. The LD3 signal is removed before detection by the photodiode (DSC50s) and oscilloscope.

wide (10% width) with a 20-ns flattop acquisition window. This window is sufficient for tests performed on the OMEGA Dante system.

For this prototype we chose to multiplex the signal from two MZM's, which was sufficient to demonstrate all concepts that will be incorporated into the final system. To further enhance the DR, the same rf signal was used to drive both MZM's. The single signal is fed to an rf splitter with a BW of 18 GHz and a 4:1 power split ratio. The asymmetric split means that the optical signal from one modulator will be 4× more sensitive to low-voltage signals, thereby extending the lower edge of the dynamic range. On the other hand, the attenuated channel can be subjected to a 4×-higher signal without exceeding $V_\pi/2$ of the modulator. Exceeding this voltage would generate a fringe jump in the sinusoidal response of the MZM. When combined, these two signals will have an enhanced DR.

The MZM's are from EOSpace and have a –3-dB EO response of between 12 GHz and 14 GHz. The modulators were chosen because they have a low V_π of 3.6 V at 1 GHz. A dc bias was applied to the MZM such that it operated quadrature point (50% transmission) with a negative slope, Q–. This gives a linear response at low voltage. Conversely, the sensitivity is low at the extrema, $V = \pm MV_\pi/2$, where M is an odd integer. In the low-signal regime, the modular sensitivity is approximately inversely proportional to V_π, so the low V_π values enhance the

DR at the lower end of the range. However, the bias points of MZM's are prone to drift with time. To maintain the operating point, a commercial monitoring circuit was employed. This circuit applied a 20-mV, 1-kHz dither to the dc bias. This dither voltage introduces harmonics of the dither frequency on the transmitted optical signal.[6] Ten percent of the light, after the MZM, is split off with a fiber-optic splitter. This signal was used to monitor the harmonics, therefore enabling the controller to maintain the Q– operating point. However, this scheme works only if the light through the MZM is cw, which it is not. Using the analog modulation capabilities of the AOM, an optical pulse shape was constructed that was at a quasi-cw level of 5% of the peak intensity. To accommodate the optical replicator, which will be described later, the cw level was turned off 2 μs before the 40-ns pulse described above was formed at the 100% transmission level. After the pulse, the AOM output was again blanked for 2 μs before returning to the 5% level. The quasi-cw light was used for the dither control. Any dither voltage that occurred during the 40-ns pulse would look like a baseline drift in the signal; therefore, the commercial controller was modified to suppress the dither voltage during the 4-μs cw blanking window.

There are two options for multiplexing the signals from the two MZM's onto a single optical fiber for additional processing and detection. A dense wavelength-division multiplexer (DWDM) with eight channels on the ITU 200 grid was used

to combine the two wavelengths. This means that in the final system, up to eight MZM's could be multiplexed onto a photo-diode attached to a single oscilloscope channel. However, the DWDM has a loss of –2.5 dB or a transmission of 56% plus two additional fiber connections with their associated losses (85% transmission). Since the prototype has only two wavelengths, a lower-loss option was to use the two inputs of the next component in the system—the optical replicator.

The optical replicator is a set of 2×2, 3-dB fused-fiber splitters, as shown in Fig. 130.90 (Ref. 7). Optical interference at the output of the fused-fiber splitters causes half of the light from each of the two input fibers to be distributed equally between the two output fibers. The splitting is independent of the wavelength over the operational band of the device. The outputs of the first 2×2 are connected to inputs of the second with an extra 12 m of fiber (60 ns) inserted into one of the connections. The output of the second 2×2 is then two identical optical pulses separated by 60 ns. The output of the second 2×2 is fed into the third 2×2 with the additional delay increased by a factor of 2 to 120 ns. This process was repeated until eight copies of the original pulse were spread over 480 ns. The input pulse cannot extend beyond 60 ns; otherwise, the tails of the pulses will overlap in time in the 2×2 splitters and produce interference with 100% modulation. This is why the AOM was configured to produce 40-ns pulses. The future version to be deployed on the NIF will require longer delays.
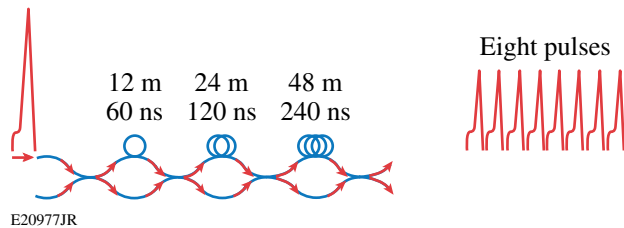

Figure 130.90
The replicator is constructed with 2×2 optical splitters. The outputs of the three stages are connected to the inputs of the subsequent stage with one of the connections having an additional length of fiber. Therefore, the eight replicated pulses arrive at the output at different times.

When detected by the photodiode, each of the optical rep-licas constitutes an independent measurement of the optical pulse from the MZM. These measurements can be averaged together to produce a measurement with the SNR improved by $\sqrt{N}$, where N is the number of replicas. For this prototype we expect an improvement in the SNR of 2.8. However, if there is any noise imprinted on the optical pulse before the replicator, e.g., noise from the LD, that noise will not average out. Since

each XRD is optically encoded with two MZM's and two LD's, any noise arising before the replicator is reduced by $\sqrt{2}$.

The replicator is a passive device, so creating eight replicas reduces the amplitude of each pulse by a factor of 8, without taking into account the coupling losses between each splitter. Therefore, increasing the number of replicas improves the SNR, but it may also decrease the signal below the detection threshold of the photodiode.

The sensitivity of the InGaAs photodiodes is approximately 0.8 A/W. When coupled into the 50-Ω input of the oscilloscope, the sensitivity can be rewritten as 40 mV/mW. At the input of the system, either 20 mW or 60 mW of optical power is available at 1552 nm or 1557 nm, respectively. In an ideal system, this power is simply gated in time and passed through to the output with analog modulation imposed. Distributing the power over eight pulses, the maximum signals that could be expected at the oscilloscope would be 100 mV and 300 mV. The system is not ideal and each component has intrinsic losses associated with it. In addition many of the components were joined together with fiber connectors rather than fusion splicing to maintain the flexibility to reconfigure the system. Table 130.IV lists the major components in the system and the associated losses in decibels (dB).

Table 130.IV: Losses in the system.

Component	Loss (dB)
Acousto-optic modulator (AOM)	–6
Polarizer	–0.6
Mach–Zehnder modulator (MZM)	–2
10/90 splitter	–1
Wavelength-division multiplexer (WDM)	–1
Miscellaneous coupling losses	–2.6
Total	–13.2

The total losses are approximately 13.2 dB or a factor of 21, which reduces the maximum-possible signals to 5 and 14 mV, respectively. Signals that are this small seriously compromise the DR of the oscilloscope measurements because they represent only a small fraction of the full-scale range, even on the most-sensitive settings. To achieve a DR of 4000:1, the optical signal must be amplified. The signal was amplified by a commercial Er-doped fiber amplifier (EDFA). This device can provide 20 db of linear gain over a wide spectral range center at 1547 nm.

The detector was a highly linear DSC50S from Discovery Semiconductor. This 50-μm detector is large with respect to the core of the optical fiber (7 μm) so it will collect all of the light from the single-mode fiber. The photodiodes have a linear response down to the dark-current limit of 10 nA. Because the system operates at the negative quadrature point of the MZM, the dark current does not affect the low-voltage sensitivity. The photodiode has a 3-dB cutoff frequency of 12 GHz.

The oscilloscope that was used to record the data was a Tektronix TDS6604 with a 6-GHz analog BW and a sampling rate of 20 GS/s, providing a temporal resolution of 50 ps. The oscilloscope has an 8-bit digitizer, nominally providing a DR of 256, which is typical for modern digitizing oscilloscopes. Unfortunately, at full BW, digitizing noise reduces this to approximately 6 bits for a DR of about 64 in single-shot mode. This is insufficient for the NIF Dante requirements and is the primary reason the optical replicas were introduced into the system.

Data-Reduction Method

Several calibration steps are necessary to convert the complicated data record at the photodetector. Figure 130.91 shows the full pulse train at the photodetector. First, the replicator output without an rf signal applied to the MZM is recorded to determine relative positions of the 16 optical pulses. The individual elements of the two sets of eight pulses are nominally identical. Their relative timing can be determined by extracting a window around each pulse and aligning the windows via a cross-correlation. These relative timings are fixed so they may be recorded for future analysis. The eight pulses, aligned in time, are then averaged together to generate an average pulse shape: $I_{J,0}(t)$. The subscript J indicates the number of the MZM. Next a small rf signal $V_{rf}(t)$ is applied to the MZM and $I_{J,rf}(t)$ is recorded along with $V_{rf}(t)$. The eight modulated pulses are then averaged together to produce a low-noise version of the MZM output. At each point in time, eight independent measurements are averaged. The standard deviation is given by the root-mean-square (rms) variation about the mean of the eight light pulses, $\Delta I_{J,opt}(t)$. The SNR at each point is easily determined as $I_{J,opt}(t)/\Delta I_{J,opt}(t)$. The MZM transmission is given by

$$I_J(t) = I_{J,0}\sin\left\{\frac{\pi\left[V_{rf}(t) + V_{J,0}\right]}{V_{J,\pi}}\right\} + I_{J,d}, \qquad (1)$$

where the parameter $V_{J,\pi}$ is the half-wave voltage, $V_{J,0}$ is the phase-equivalent, bias-point voltage, and $I_{J,d}$ is the combined optical leakage and bias. These values are approximately

known. The manufacturer specifies $V_{J,\pi}$. The $Q-$ operating point implies $V_{J,0}$ is $1.5 \times V_\pi$ and $I_{J,d} \sim I_{J,0}$. For $V_{rf}(t) \ll V_{J,\pi}$, the response is essentially linear and Eq. (1) can be easily inverted over a time window that encompasses the flattop portion of the optical pulse without having to account for multifringe effects. The clean, optically measured $V_{rf}(t)$ can then be compared with the applied, electronically measured $V_{rf}(t)$ and cross-correlated to determine the relative phase. Using the averaged pulse shape makes it less likely that the cross-correlation will be biased by noisy data. Once the temporal alignment is established, the magnitude of $V_{rf}(t)$ can be increased to values greater than $V_\pi/2$ to map out the entire transmission function. The algorithm specified in IEEE standard 1240 (Ref. 8) is used to determine the best-fit values for the constants for the system calibration. Each MZM is now calibrated with a baseline optical transmission curve and three scalar constants. The system is now ready to measure arbitrary rf signals.
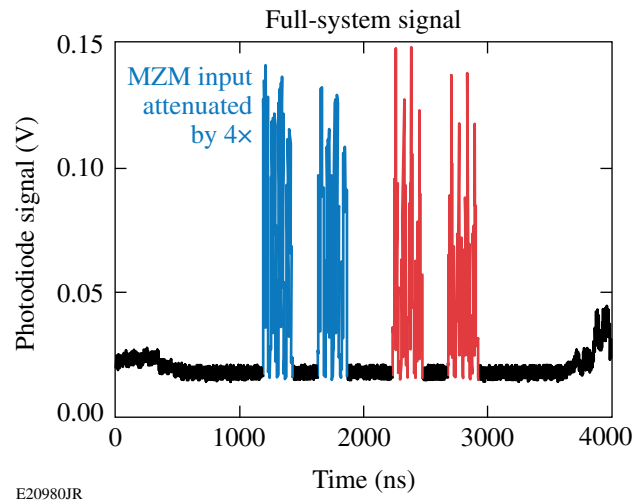

Figure 130.91
The optical signal detected at the oscilloscope at the output of the instrument has 16 serially combined pulses, eight from each Mach–Zehnder modulator (MZM).

The baseline optical transmission with $V_{rf}(t) = 0$ should be reacquired shortly before the actual data are taken to account for drifts in the performance of the many EO components in the system. The arbitrary rf signal is then measured. The eight pulses from the MZM with highest attenuation ($J = 1$, $\lambda_1 = 1557$ nm) are averaged and then converted using calibrated sinusoidal transmittance of the modulator. Ideally, the attenuation is set such that the voltage applied to MZM$_1$ never exceeds $V_{1,\pi}$. The unfolded $V_{1,rf}(t)$ from the first MZM is used in conjunction with the calibrated $V_{2,\pi}$ of the lowest-attenu-

ation MZM to determine when the voltage applied to MZM_2 exceeded $V_{2,\pi}/2$. Normally, the arcsine function is calculated on the interval from $(M + 1/2)\pi$ to $(M + 1.5)\pi$, where M is an integer. Note that the sign flips between adjacent intervals. By noting whether M is even or odd, the multivalued unfolding can be made unambiguously single valued.

The averaged and unfolded signals from the two MZM's can be cross-correlated to determine the temporal alignment. The next step is to combine the two EO measured signals. As described above, the SNR can be calculated at each temporal point of the two waveforms. These SNR's can be quite different between the two curves, particularly when MZM_2 reaches the vicinity of $V_{2,\pi}/2$. The slope of the transmission function is zero at this point. The unfolding function has the form

$$V_{\rm rf}(t) = \frac{V_{J,\pi}}{\pi} \sin^{-1}\left[\frac{I_J(t) - I_{J,d}}{I_{J,0}}\right] - V_{J,0}. \qquad (2)$$

Taking the derivative with respect to $I_{\rm opt}$ and multiplying by $\Delta I_{\rm opt}(t)$, the standard deviation of the optical measurements at each point, the variation in $V_{\rm rf}(t)$ as a function of $I_{\rm opt}(t)$ and $\Delta I_{\rm opt}(t)$ can be determined.

$$\Delta V_{J,\rm rf}(t) = \Delta I_J(t)\frac{{\rm d}V_{J,\rm rf}}{{\rm d}I_J} = \frac{V_{J,\pi}\Delta I_J(t)}{I_{J,0}\pi\sqrt{1 - \left[\frac{I_J(t) - I_{J,d}}{I_{J,0}}\right]^2}}, \qquad (3)$$

when $V_{\rm rf}(t)$ equals $V_{J,\pi}/2$, $I_{J,\rm opt}(t)$ is approximately zero, and the derivative diverges. Small errors in the measurement $\Delta I_{J,\rm opt}(t)$ lead to large changes in the variation of the EO measured rf voltage $\Delta V_{J,\rm rf}(t)$. A weighted average based on standard deviations of the two signals was used to combine the two MZM's. To calculate the standard deviation, the rms deviation of the light pulses $\Delta I_{J,\rm opt}(t)$, was fed into Eq. (2) as

$$I_{J,\rm opt^+}(t) = I_{J,\rm opt}(t) + \Delta I_{J,\rm opt}(t) \qquad (4a)$$

and

$$I_{J,\rm opt^-}(t) = I_{J,\rm opt}(t) - \Delta I_{J,\rm opt}(t). \qquad (4b)$$

These substitutions generated $\Delta V_{J,\rm rf^+}(t)$ and $\Delta V_{J,\rm rf^-}(t)$, respectively. The rms variation in $V_{J,\rm rf}(t)$ was then defined as

$$\Delta V_{J,\rm rf}(t) = \left[\Delta V_{J,\rm rf^+}(t) + \Delta V_{J,\rm rf^-}(t)\right]/2. \qquad (5)$$

The weighting function for the averaging was taken as the inverse of the standard deviation of the raw data $1/\Delta I_{J,\rm opt}(t)$ normalized by the sum of all the weights:

$$W_J(t) = \left[1/\Delta I_{J,\rm opt}(t)\right]\Big/\sum\left[1/\Delta I_{J,\rm opt}(t)\right]; \qquad (6)$$

$$\langle V_{\rm rf}(t)\rangle = \sum\left[V_{J,\rm rf}W_J(t)\right]. \qquad (7)$$

Likewise, the final rms variation at each point is the weighted rms sum or the variations from each modulator:

$$\Delta\langle V_{\rm rf}(t)\rangle = \sqrt{\sum \Delta V_{J,\rm rf}(t)\Delta V_{J,\rm rf}(t)W_J(t)} \qquad (8)$$

and the SNR is $\langle V_{\rm rf}(t)\rangle\big/\Delta\langle V_{\rm rf}(t)\rangle$.

With the hardware and signal-processing algorithms in place, the system was incorporated into the Dante instrument on LLE's OMEGA laser. An rf splitter was used to tap off half of the signal feeding one of the Dante SCD5000 transient digitizers. In this way we could directly compare the current system and the prototype. Figure 130.92 shows the averaged optical output of the two MZM's. Each averaged output is bracketed by curves representing +1 and –1 standard deviation. The data from the highly attenuated modulator vaguely resemble an inverted copy of the output of the XRD. The low-attenuation MZM output is highly distorted because the voltage exceeded $V_\pi/2$. This signal required the unfolded signal from the highly attenuated MZM to remove the multivalue ambiguities. This procedure is fully automated. Figure 130.93 shows the combined average of the two MZM's and the purely electrical measurement from the SCD5000. The average rms difference between the two waveforms is 2.6%. Another way to compare the measurements from the different instruments is to look at the spectral content. Figure 130.94 shows the fast Fourier transform (FFT) of both waveforms. The spectra match out to a frequency of about 3.5 GHz. The rise time of the XRD's is approximately 120 ps, giving a maximum frequency of 2.75 GHz. Therefore, we expect the EO acquisition system to capture all of the frequency delivered by the XRD.
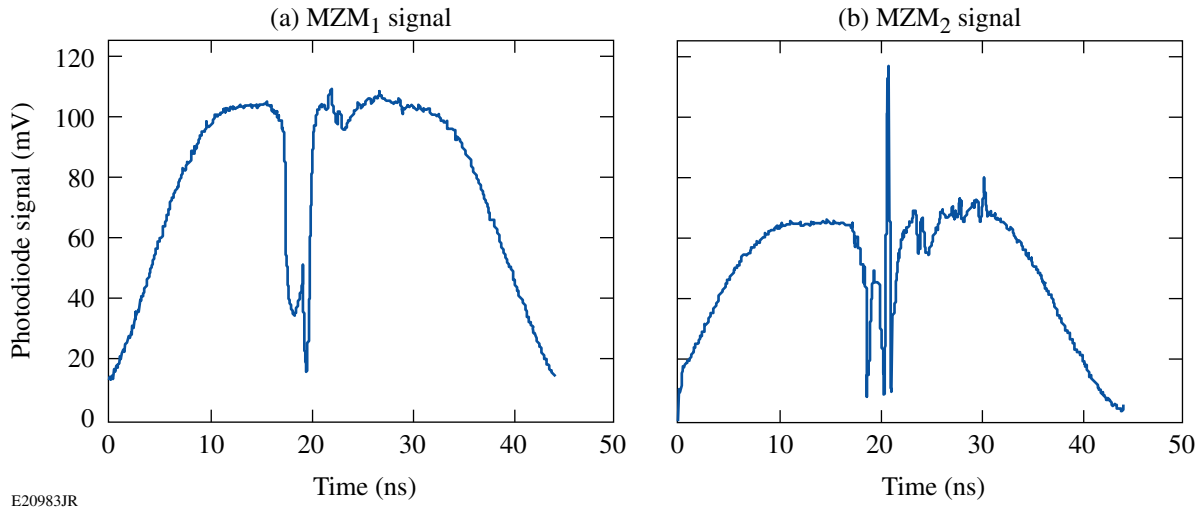
Using an offline electronic pulse generator to simulate the NIF Dante XRD's, signals as large as 18 V were measured with the prototype system. Using the analysis described above, the SNR was calculated and is plotted against unfolded and averaged signals in Fig. 130.95. The peak SNR was approximately 500:1. The horizontal line is at an SNR of 1 and represents the minimum signal detectable by the instrument. The measured

points cross this line at 30 mV, so the demonstrated DR is 600:1. The relevance of Fig. 130.95 is illustrated in Fig. 130.96, where the system output for a 30-mV input pulse is plotted. The output is very noisy and just barely discernible.

Conclusions

A prototype EO acquisition system, the NIF Dante, has been built and tested. The system has a DR of 600:1 and a peak SNR of 500:1. The prototype has demonstrated that the concept
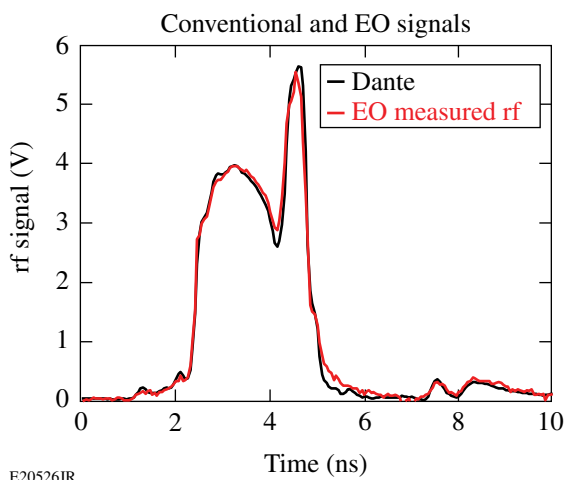
works, but not all of the specifications of the NIF Dante upgrade have been met. In particular, the DR demonstrated so far is too small. On the high end, the maximum signal is limited to the voltage that drives both MZM's beyond $V_\pi/2$. At that point the automated reduction routines cannot define a unique unfolding. The solution to this problem is to add an additional MZM with still-higher attenuation on its rf input. Other strategies must be employed to reach an SNR of 5 at a signal of 50 mV over a 200-ps interval. We now have an SNR of 1 at 30 mV over
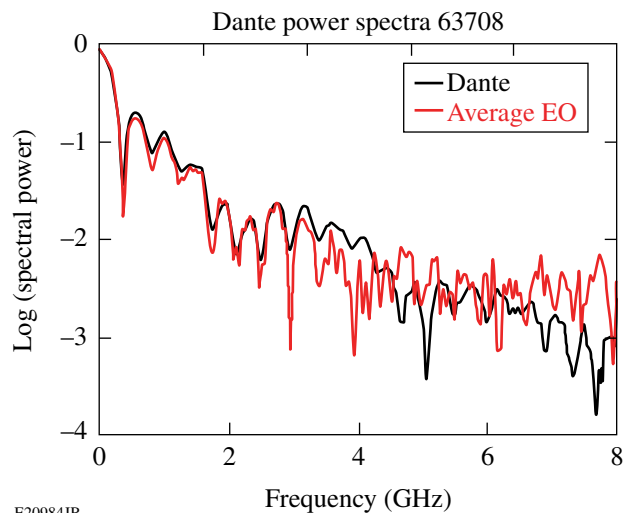

Figure 130.92
The averaged output of the two MZM's. (a) The signal from MZM_1 is approximately an inverted replica of the radio frequency (rf) input. (b) The signal from MZM_2 is highly distorted as a result of fringe shifts.

Figure 130.93
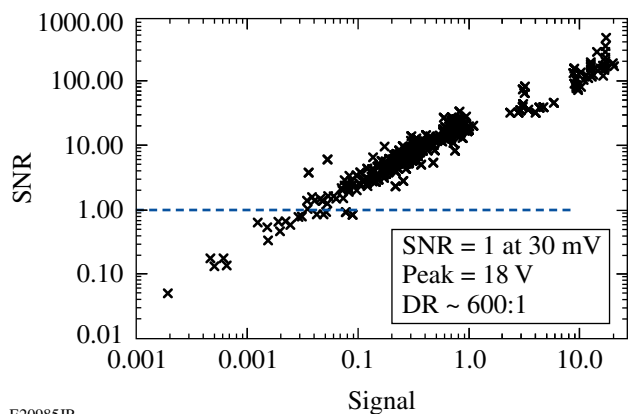The electro-optic (EO) measurement agrees with that of a high-dynamic-range digitizer.
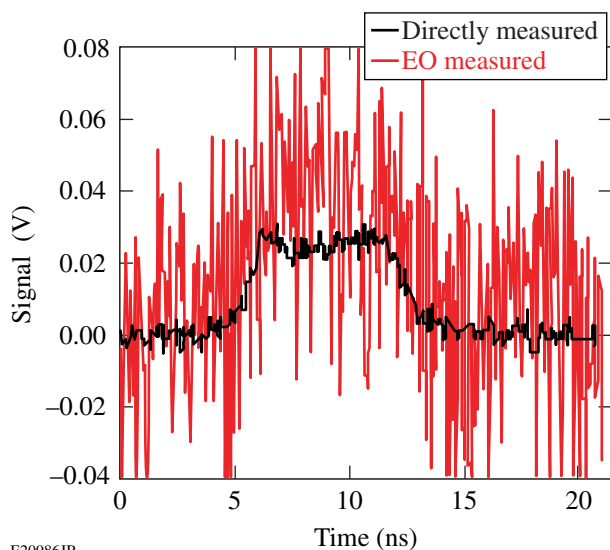
Figure 130.94
The frequency content of the SCD5000 and the EO measurements match out to 3.75 GHZ, which is greater than the bandwidth of the x-ray photodiode.

E20985JR

Figure 130.95

The signal-to-noise ratio (SNR) plotted against the EO measured signal clearly shows that the minimum-detectable signal occurs at 30 mV, where the SNR crosses the horizontal line. The DR is ~600:1.

E20986JR

Figure 130.96

At 30 mV, the EO measured output (red curve) is noisy with respect to the directly measured radio frequency (black curve).

a 50-ps time interval. Figure 130.95 implies an SNR of 1.7 at 50 mV. Averaging four points to get to the 200-ps interval will improve the SNR by a factor of 2, giving an SNR of 3.4, which almost meets the specification. The number of replicas can probably be increased to 32 without adding an undue burden of optical fiber management on the system. This will increase the SNR by a factor of 2, and, therefore, will meet the specification. Using a 12-GHz, 40-GS/s oscilloscope will accomodate an eight-point temporal smoothing that could increase the SNR by $\sqrt{8}$. Beyond that, it will be necessary to explore using quieter lasers and an EDFA with lower noise figures.

ACKNOWLEDGMENT

REFERENCES

1. E. I. Moses, Fusion Sci. Technol. **54**, 361 (2008).

2. E. L. Dewald *et al.*, Rev. Sci. Instrum. **75**, 3759 (2004).

3. E. L. Wooten *et al.*, IEEE J. Sel. Top. Quantum Electron. **6**, 69 (2000).

4. *Generic Reliability Assurance Requirements for Optoelectronic Devices Used in Telecommunications Equipment*, Telcordia Technologies, Inc., Piscataway, NJ, Document No. GR-468-CORE, Issue 2 (September 2004).

5. Fiberdyne Labs, Inc., accessed 26 April 2012, http://www.fiberdyne.com/products/itu-grid.html.

6. E. I. Ackerman and C. H. Cox III, in *International Topical Meeting on Microwave Photonics, 2000* (IEEE, New York, 2000), pp. 121–124.

7. W. R. Donaldson, J. R. Marciante, and R. G. Roides, IEEE J. Quantum Electron. **46**, 191 (2010).

8. *IEEE Std. 1241-2000, IEEE Standard for Terminology and Test Methods for Analog-to-Digital Converters* (IEEE, New York, 2001).